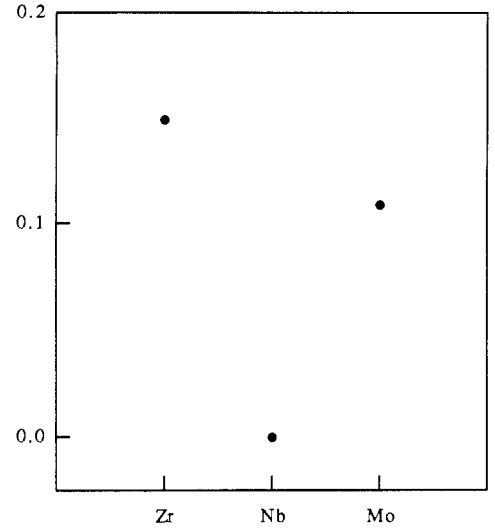

Figure 6. Plot of M-M distances in the three $M_2Cl_6(dppe)_2$ compounds corrected for the relative radii of the metal atoms (see text).

tained might well be attributed to the fact that the disposition of ligands found in the $Zr_2Cl_6(PEt_3)_4(C_2H_4)$ molecule, shown schematically as I, cannot be obtained when the pairs of phos-

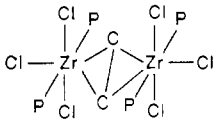

I

phorus atoms are tied together by the dimethylene bridge. This, however, does not provide a wholly satisfactory explanation for the lack of reactivity of $Zr_2Cl_6(dppe)_2$ toward 1,2-$C_2H_4Cl_2$. We have previously suggested that the reaction of 1,2-$C_2H_4Cl_2$ with $Zr_2Cl_6(PR_3)_4$ compounds proceeds according to eq 1, although

$$2Zr_2Cl_6(PR_3)_4 + C_2H_4Cl_2 \rightarrow Zr_2Cl_6(PEt_3)_4(C_2H_4) + 2ZrCl_4(PEt_3)_2 \quad (1)$$

we have not conclusively demonstrated the formation of $ZrCl_4(PEt_3)_2$. It is not obvious why $Zr_2Cl_6(dppe)_2$ could not react with 1,2-$C_2H_4Cl_2$ according to eq 2. Clearly, the chemistry of these dinuclear zirconium(III) compounds requires further study.

$$Zr_2Cl_6(dppe)_2 + C_2H_4Cl_2 \rightarrow 2ZrCl_4(dppe)_2 + C_2H_4 \quad (2)$$

A formal point to be noted here in comparing the structural parameters collected in Table VIII is that the Zr-P distances in the three $Zr_2Cl_6(PR_3)_4$ compounds show a variation, whereas all the Zr-Cl distances are essentially identical. We shall not attempt to reconcile the Zr-P distances in $Zr_2Cl_6(dppe)_2$ with those in the other compounds since the P-Zr-P angle is so very different and this might have a serious but unpredictable effect on the Zr-P bond strengths. We therefore compare only the last three compounds in Table VIII. We first note that statistically there is little significance to the apparent difference between the Zr-P distances in the PEt_3 and PBu_3 cases. It is not significant at the commonly used 3σ level since it and its esd are 0.021 [8] Å. However, between the value in the PMe_2Ph compound and the average of those in the other two compounds, there is a significant difference of 0.068 [8] Å. The shorter Zr-P bond in the PMe_2Ph compound indicates that this phosphine is a better donor (stronger Lewis base) than the trialkylphosphines. This order of basicity is in accord with the results of previous studies,[24,25] which have shown that, contrary to expectation from simple inductive arguments, phosphine basicity increases in the order $PMe_3 < PMe_2Ph < PMePh_2$.

Acknowledgment. We thank the Robert A. Welch Foundation for support. M.P.D. thanks the National Science Foundation for a NSF Predoctoral Fellowship and Texaco/IUCCP for additional support.

Registry No. 1, 112571-00-3; **2**, 112421-71-3; **3**, 77061-31-5; $ZrCl_4$, 10026-11-6; Zr, 7440-67-7.

Supplementary Material Available: Full listings of bond distances, bond angles, and isotropic equivalent displacement parameters for $Zr_2Cl_6(dppe)_2 \cdot 2C_2H_4Cl_2 \cdot 1.5C_6H_5CH_3$ (**1**), $Zr_2Cl_6(PMe_2Ph)_4$ (**2**), and $Zr_2Cl_6(PEt_3)_4$ (**3**) (13 pages); listings of observed and calculated structure factors for **1-3** (46 pages). Ordering information is given on any current masthead page.

(24) Puddephatt, R. J.; Bancroft, G. M.; Chan, T. *Inorg. Chim. Acta* **1983**, *73*, 83.
(25) Bancroft, G. M.; Dignard-Bailey, L.; Puddephatt, R. J. *Inorg. Chem.* **1986**, *25*, 3675.

Contribution from the Department of Chemistry and Laboratory for Molecular Structure and Bonding, Texas A&M University, College Station, Texas 77843

Oxidative-Addition Reactions of S-S and Se-Se Bonds to Mo_2 and W_2 Quadruple Bonds

Jo Ann M. Canich, F. Albert Cotton,* Kim R. Dunbar, and Larry R. Falvello

Received September 30, 1987

Oxidative-addition chemistry of the quadruply bonded molybdenum and tungsten $M_2Cl_4(dppm)_2$ dimers (dppm = bis(diphenylphosphino)methane) has been investigated by using diphenyl disulfide, diphenyl diselenide, dichloromethane, and chlorine as the oxidizing agents. The products to be discussed here are the following: $W_2(\mu\text{-SPh})_2Cl_4(dppm)_2$ (**1**), $W_2(\mu\text{-SPh})(\mu\text{-Cl})Cl_4(dppm)_2$ (**2**), $W_2(\mu\text{-SePh})_2Cl_4(dppm)_2$ (**3**), $W_2(\mu\text{-SePh})(\mu\text{-Cl})Cl_4(dppm)_2$ (**4**), $W_2(\mu\text{-Cl})_2Cl_4(dppm)_2$ (**5**), $Mo_2(\mu\text{-SPh})(\mu\text{-Cl})Cl_4(dppm)_2$ (**6**), and $Mo_2(\mu\text{-Cl})_2Cl_4(dppm)_2$ (**7**). The structural characterization of compounds **1**, **4**, and **6** is reported here. Pertinent crystal data are as follows: **1**, $P\bar{1}$, a = 12.991 (2) Å, b = 13.851 (3) Å, c = 11.693 (2) Å, α = 111.28 (2)°, β = 103.43 (2)°, γ = 89.03 (2)°, V = 1903 (1) Å^3, W-W = 2.787 (1) Å; **4**, $Pna2_1$, a = 39.335 (10) Å, b = 15.371 (4) Å, c = 11.774 (3) Å, V = 7119 (5) Å^3, W-W = 2.708 (2) Å; **6**, $P2_1/n$, a = 12.096 (4) Å, b = 24.474 (6) Å, c = 23.329 (5) Å, β = 100.73 (2)°, V = 6786 (3) Å^3, Mo-Mo = 2.788 (1) Å.

Introduction

Previous reports from this laboratory have established the synthetic utility of oxidative-addition reactions in which reagents such as halogens, X_2, or disulfides, RSSR, react with M-M multiple bonds to give products in which the M-M bond order is reduced and X or RS groups serve as bridging ligands. The first examples were those in which $M_2Cl_4(dto)_2$ and $Mo_2Cl_4(dmpe)_2$ [dto = 3,6-dithiaoctane and dmpe = 1,2-bis(dimethylphosphino)ethane] reacted with diethyl disulfide to form $Mo_2(\mu\text{-SEt})_2Cl_4(dto)_2$ and $Mo_2(\mu\text{-SEt})_2Cl_4(dppe)_2$, respectively.[1] The formation of small amounts of $Mo_2(\mu\text{-Cl})_2Cl_4(dto)_2$ from $Mo_2Cl_4(dto)_2$ dissolved in dichloromethane[2] probably represents

(1) (a) Cotton, F. A.; Powell, G. L. *J. Am. Chem. Soc.* **1984**, *106*, 3372. (b) Cotton, F. A.; Diebold, M. P.; O'Connor, C. J.; Powell, G. L. *J. Am. Chem. Soc.* **1985**, *107*, 7438.

0020-1669/88/1327-0804$01.50/0

the first observation of CH_2Cl_2 serving as a source of two chlorine atoms in this particular type of chemistry, although its ability to do so is more generally established. Reactions of Cl_2 with $Mo_2Cl_4(P\text{-}P)_2$ [P-P = (dimethylphosphino)methane (dmpm), 1,2-bis(diphenylphosphino)ethane (dppe)] and $W_2Cl_4(P\text{-}P)_2$ [P-P = bis(diphenylphosphino)methane (dppm), dppe] to form $(\mu\text{-}Cl)_2$ products have more recently been reported,[3] and the reaction of $Re_2Cl_4(dppm)_2$ with PhSeSePh has also been shown to give $Re_2(\mu\text{-}SePh)_2Cl_4(dppm)_2$.[4]

Apart from the two examples cited above, studies of oxidative-addition reactions of W–W quadruple bonds for designed synthesis have not previously been reported. Since the W_2^{4+} moiety is considerably more susceptible to oxidation than the Mo_2^{4+} unit, as evidenced by several unintended reactions,[5,6] we felt that such a study would be rewarding. A study of the reactions of $W_2Cl_4(dppm)_2$ and also $Mo_2Cl_4(dppm)_2$ in several solvents is described here. The oxidative reagents employed were PhSSPh, PhSeSePh, Cl_2, and CH_2Cl_2.

Experimental Procedures

Because of the air sensitivity of $W_2Cl_4(dppm)_2$, standard Schlenk and vacuum-line techniques were used in the preparation of all tungsten-containing compounds. Toluene, tetrahydrofuran, and benzene were freshly distilled from benzophenone ketyl, and dichloromethane was distilled from P_4O_{10}. All solutions were transferred by use of stainless steel cannulas and/or syringes. $W_2Cl_4(dppm)_2$ and $Mo_2Cl_4(dppm)_2$ were prepared by literature methods.[7] Bis(diphenylphosphino)methane, diphenyl disulfide, and diphenyl diselenide were purchased from Aldrich Chemical Co. Dichloromethane was obtained from Fisher Scientific Co.

Infrared and visible spectra were recorded on Perkin-Elmer 783 and Cary 17D spectrophotometers, respectively. IR spectra were obtained as Nujol mulls between CsI plates, and peaks coincident with Nujol are not reported. Samples for the visible spectra were contained in glass cells equipped with Teflon-coated septa and having a path length of 1 cm. No attempt was made to determine extinction coefficients.

Preparation of $W_2(SPh)_2Cl_4(dppm)_2$ (1). A solution of $W_2Cl_4(dppm)_2$ (0.10 g, 0.078 mmol) in 25 mL of toluene was filtered into a 100-mL round-bottom Schlenk flask containing 0.0191 g (0.087 mmol) of PhSSPh. The reaction mixture was gently heated with stirring until a deep cherry red solution developed (~0.5 h). Note that overheating decomposes the reaction product. The resulting solution was refiltered, and the solvent was removed by vacuum distillation. The solid was washed with two 5-mL portions of hexane and then pumped to dryness. The bright red powder, $W_2(SPh)_2Cl_4(dppm)_2$, was recovered in 58% yield. $W_2(SPh)_2Cl_4(dppm)_2$ is an air-stable solid, but solutions are air-sensitive. IR (Nujol/CsI, cm^{-1}): 1573 (w), 1435 (s), 1307 (br, vw), 1192 (w), 1160 (w), 1132 (w), 1098 (m), 1074 (w), 1026 (w), 1003 (w), 973 (br, w), 922 (br, vw), 843 (br, w), 783 (m), 741 (s), 729 (sh, m), 695 (s), 622 (w), 526 (m), 514 (m), 489 (m), 464 (w), 426 (w), 375 (br, w), 357 (w), 329 (m), 319 (m), 305 (m). Visible (toluene, nm): 504 (s), 730 (w).

Crystallization of $W_2(SPh)_2Cl_4(dppm)_2$ (1). X-ray crystallographic crystals of $W_2(SPh)_2Cl_4(dppm)_2$ were grown by placing a layer of hexane solvent over a solution of the reaction mixture. Slow diffusion of layers allowed for growth of block-shaped red crystals.

Preparation of $W_2(SPh)Cl_5(dppm)_2$ (2). Method 1. The compound $W_2Cl_4(dppm)_2$ (0.10 g, 0.078 mmol) was dissolved in 20 mL of CH_2Cl_2 and filtered into a 100-mL round-bottom Schlenk flask containing 0.0191 g (0.087 mmol) of PhSSPh. The mixture was heated with stirring for 10 min to give an orange-brown solution containing a mixture of $W_2Cl_6(dppm)_2$ and $W_2(SPh)Cl_5(dppm)_2$ as determined by visible spectroscopy. Visible for $W_2Cl_6(dppm)_2$ (CH_2Cl_2, nm): 465 (s), 384 (w). Visible for $W_2(SPh)Cl_5(dppm)_2$ (CH_2Cl_2, nm): 435 (s).

Method 2. In a 100-mL Schlenk tube was dissolved 0.05 g (0.033 mmol) of $W_2(SPh)_2Cl_4(dppm)_2$ in 10 mL of CH_2Cl_2. Over a period of 1 day, the solution reacted to form a mixture of $W_2(SPh)Cl_5(dppm)_2$ and $W_2Cl_6(dppm)_2$, as determined by visible spectroscopy.

Crystallization of $W_2(SPh)Cl_5(dppm)_2$ (2). A fresh solution of **2**, prepared as above, was placed in an Erlenmeyer flask along with 10 mL of hexane. Slow evaporation of the solution in air provided small red-brown needles that diffracted poorly.

Preparation of $W_2(SePh)_2Cl_4(dppm)_2$ (3). A filtered solution of 0.010 g (0.078 mmol) of $W_2Cl_4(dppm)_2$ dissolved in 25 mL of toluene was added to a 100-mL round-bottom Schlenk flask containing 0.025 g (0.080 mmol) of PhSeSePh. The reaction mixture was gently heated for 0.5 h or until a purple solution developed. The solution was pumped to dryness, and the solids were washed with two 10-mL portions of hexane to leave a residue of $W_2(SePh)_2Cl_4(dppm)_2$ in 45% yield. $W_2(SePh)_2Cl_4(dppm)_2$ is an air-stable solid, but solutions are air-sensitive. IR (Nujol/CsI, cm^{-1}): 1585 (w), 1571 (w), 1438 (m), 1308 (br, w), 1267 (br, w), 1192 (w), 1162 (w), 1130 (w), 1096 (br, m), 1030 (sh, w), 1023 (w), 1004 (w), 976 (br, w), 847 (w), 790 (br, m), 740 (s), 695 (s), 623 (w), 528 (s), 514 (s), 489 (m), 425 (m), 377 (w), 322 (br, w), 304 (m). Visible (toluene, nm): 502 (s), 720 (w).

Preparation of $W_2(SePh)Cl_5(dppm)_2$ (4). Method 1. The compound $W_2Cl_4(dppm)_2$ (0.10 g, 0.078 mmol) was dissolved in 20 mL of CH_2Cl_2 and filtered into a 100-mL Schlenk flask containing 0.025 g (0.080 mmol) of PhSeSePh. The reaction mixture was stirred at room temperature for 1 day, yielding an orange-brown solution. Upon removal of the solvent, $W_2(SePh)Cl_5(dppm)_2$ could be isolated in 55% yield. Visible (CH_2Cl_2, nm): 430 (s).

Method 2. The compound $W_2(SePh)_2Cl_4(dppm)_2$ was dissolved in 10 mL of CH_2Cl_2 and filtered into a 100-mL Schlenk tube. Over a period of 1 day, the solution reacted to form $W_2(SePh)Cl_5(dppm)_2$ and $W_2Cl_6(dppm)_2$ as evidenced by visible spectroscopy.

Crystallization of $W_2(SePh)Cl_5(dppm)_2$ (4). X-ray-quality crystals of $W_2(SePh)Cl_5(dppm)_2$ were grown from 10 mL of a filtered reaction solution as described above (method 1), which was layered with 10 mL of hexane in a Schlenk tube. Slow diffusion resulted in the growth of small needle-shaped orange-brown crystals, which were structurally characterized by X-ray diffraction.

Preparation of $Mo_2(SPh)Cl_5(dppm)_2$ (6). In a typical reaction, $Mo_2Cl_4(dppm)_2$ (0.20 g, 0.181 mmol) and PhSSPh (0.20 g, 0.92 mmol) were stirred together at room temperature in CH_2Cl_2 (15 mL). The progress of the reaction was monitored by UV–visible spectroscopy according to the disappearance of the $\delta \rightarrow \delta^*$ transition of $Mo_2Cl_4(dppm)_2$. The initial green solution gradually turned to amber, and after 7 days the reaction was judged to be complete. The solution was filtered to give a small amount of brown solid and an amber filtrate, which was reduced in volume to ca. 10 mL. Hexane (50 mL) was added to induce precipitation, and the crude brown material was filtered off and washed with diethyl ether to remove excess PhSSPh. The solid dissolved partially in benzene to give a bright red solution and an insoluble yellow powder. The red benzene solution was evaporated to a residue, which was taken up in 5 mL of CH_2Cl_2 and layered with a THF/benzene mixture (50/50). Slow evaporation of the solution under argon led to the formation of dark red crystals of $Mo_2(SPh)Cl_5(dppm)_2$, yield 0.020 g (~8%). UV–visible (CH_2Cl_2, nm): 325 (s), 426 (s). On the basis of its visible spectrum, the benzene-insoluble yellow solid appears to be a mixture of compounds. Two absorptions at 435 and 460 nm vary in intensity from one experiment to another and for different workup procedures. When the reaction is carried out under reflux conditions, the reaction times are much shorter (3–4 days in CH_2Cl_2, 10–12 h in toluene). The product isolated from refluxing toluene in an orange-brown microcrystalline material with IR and electronic spectral properties that indicate it is a single compound. The limited solubility of the product precludes the use of elemental analysis in the determination of the molecular formula, since we cannot be certain of the purity of an unrecrystallized sample. Unfortunately we have been unsuccessful in our attempts to grow single crystals of the compound and so its density remains uncertain. IR (Nujol/CsI, cm^{-1}): 1575 (w), 1565 (w), 1295 (w), 1140 (m), 1100 (s), 1065 (m), 1020 (w), 992 (w), 970 (m), 840 (w), 775 (m), 735 (s), 720 (m), 685 (s), 580 (m), 550 (w), 500 (m), 480 (m), 380 (w), 350 (m), 320 (w). Visible (CH_2Cl_2, nm): 370 (s), 450 (w).

Preparation of $Mo_2Cl_6(dppm)_2$ (7). A sample of $Mo_2Cl_4(dppm)_2$ (0.20 g, 0.181 mmol) was treated with approximately 1 equiv of $Cl_2(g)$ (5–6 mL) in 25 mL of CH_2Cl_2. The green solution instantly turned bright red, and pink-red crystals began forming on the sides and bottom of the flask. The volume of the solution was reduced to ca. 5 mL, and the crystalline product was filtered off and washed with diethyl ether; yield 0.20 g (95%). The compound was characterized by a comparison of its IR and UV/visible spectral features with those obtained for a sample of the authentic fully characterized complex.[8] Visible (CH_2Cl_2, nm): 400 (s), 532 (s).

(2) Cotton, F. A.; Fanwick, P. E.; Fitch, J. W. *Inorg. Chem.* **1978**, *17*, 3254.
(3) (a) Canich, J. M.; Cotton, F. A.; Daniels, L. M.; Lewis, D. B. *Inorg. Chem.* **1987**, *26*, 4046. (b) Chakravorty, A. R.; Cotton, F. A.; Diebold, M. P.; Lewis, D. B.; Roth, W. J. *J. Am. Chem. Soc.* **1986**, *108*, 971. (c) Agaskar, P. A.; Cotton, F. A.; Dunbar, K. R.; Falvello, L. R.; O'Connor, C. J. *Inorg. Chem.* **1987**, *26*, 4051.
(4) Cotton, F. A.; Dunbar, K. R. *Inorg. Chem.* **1987**, *26*, 1305.
(5) Cotton, F. A.; Mott, G. N. *J. Am. Chem. Soc.* **1982**, *104*, 5978.
(6) Fanwick, P. E.; Harwood, W. S.; Walton, R. A. *Inorg. Chem.* **1987**, *26*, 242.
(7) (a) Canich, J. M.; Cotton, F. A. *Inorg. Chim. Acta* **1988**, *142*, 69. (b) Best, S. A.; Smith, T.J.; Walton, R. A. *Inorg. Chem.* **1978**, *17*, 99.
(8) Carmona, E.; Galindo, A.; Sanchez, L.; Nielson, A. J.; Wilkinson, G. *Polyhedron* **1984**, *3*, 347.

Table I. Crystal Data for $W_2(SPh)_2Cl_4(dppm)_2 \cdot 3C_7H_8$ (**1**), $W_2(SePh)Cl_5(dppm)_2 \cdot 3CH_2Cl_2$ (**4**), and $Mo_2(SPh)Cl_5(dppm)_2 \cdot {}^1/_2CH_2Cl_2 \cdot OC_4H_8 \cdot C_6H_6$ (**6**)

	1	**4**	**6**
formula	$W_2Cl_4S_2P_4C_{83}H_{78}$	$W_2SeCl_{11}P_4C_{61}H_{55}$	$Mo_2Cl_6SP_4OC_{66.5}H_{64}$
fw	1773.1	1748.6	1439.8
space group	$P\bar{1}$	$Pna2_1$	$P2_1/n$
systematic absences	none	$0kl$ ($k + l \neq 2n$), $h0l$ ($h \neq 2n$)	$h0l$ ($h + l \neq 2n$), $0k0$ ($k \neq 2n$)
a, Å	12.991 (2)	39.335 (10)	12.096 (4)
b, Å	13.851 (3)	15.371 (4)	24.474 (6)
c, Å	11.693 (2)	11.774 (3)	23.329 (5)
α, deg	111.28 (2)	90	90
β, deg	103.43 (2)	90	100.73 (2)
γ, deg	89.03 (2)	90	90
V, Å^3	1902 (1)	7119 (5)	6786 (3)
Z	1	4	4
d_{calcd}, g/cm^3	1.548	1.631	1.409
cryst size, mm	0.1 × 0.1 × 0.2	0.2 × 0.3 × 0.5	0.25 × 0.30 × 0.40
μ(Mo Kα or Cu Kα), cm^{-1}	85.527	43.460	7.603
data collecn instrum	Syntex P$\bar{1}$	Syntex P3	Syntex P$\bar{1}$
radiation (monochromated in incident beam)	Cu Kα (λ_α = 1.540 56 Å)	MoK$_\alpha$ (λ_α = 0.710 73 Å)	MoKα (λ_α = 0.710 73 Å)
orientation rflcns: no.; range (2θ), deg	15; $2\theta > 45$	25; 17.5–30.6	15; 20.9–37.7
temp, °C	20	20	0
scan method	ω–2θ	ω	ω–2θ
data collecn range, 2θ, deg	3–115	4–45	4–50
no. of unique data, total with $F_o^2 > 3\sigma(F_o^2)$	6966, 4791	7302, 3366	6699, 5678
no. of params refined	382	277	657
transmission factors: max, min	1,000, 0.686		0.9972, 0.2825
R^a	0.0501	0.0738	0.0666
$R_w{}^b$	0.0638	0.0709	0.0965
quality-of-fit indicator^c	1.294	1.39	1.797
largest shift/esd, final cycle	0.03	0.84	0.23
largest peak, e/Å^3	1.454	1.600	1.046

$^a R = \sum||F_o| - |F_c||/\sum|F_o|$. $^b R_w = [\sum w(|F_o| - |F_c|)^2/\sum w|F_o|^2]^{1/2}$; $w = 1/\sigma^2(|F_o|)$. ^{c} Quality of fit = $[\sum w(|F_o| - |F_c|)^2/(N_{observns} - N_{params})]^{1/2}$.

Crystallography. All samples were mounted in a protected environment either by coating the crystal with epoxy resin and mounting it on the end of a glass fiber or by sealing the crystal in a glass capillary tube with epoxy resin. Single-crystal diffraction experiments were conducted by using either a Syntex P$\bar{1}$ or P3 automated four-circle X-ray diffractometer equipped with monochromated Mo Kα radiation. The data for compound **1** were obtained at Crystalytics on a Syntex P$\bar{1}$ diffractometer using Cu Kα radiation. Routine unit cell identification and intensity data collection procedures were followed. These have been fully described elsewhere.[9] Photographs of the principal axes were taken to verify symmetry and lattice dimensions and to ascertain crystal quality. Three check reflections were used to monitor gain or loss of intensity throughout the data collection. Lorentz, polarization, and empirical absorption corrections based on azimuthal scans[10] were applied to all data sets. Standard computational procedures were used to solve and refine structures by using either the VAX-SDP software package or SHELX on VAX-11/780, MicroVAX II, and/or 8650/8800 VAX Cluster computer systems. Pertinent crystallographic parameters for the crystal structures are summarized in Table I.

Structure Solution and Refinement for $W_2(SPh)_2Cl_4(dppm)_2 \cdot 3C_7H_8$ (1). The unique tungsten atom was located from the Patterson map. The centrosymmetric space group $P\bar{1}$ was chosen and led to the correct solution. A series of alternating least-squares refinements and difference Fourier maps led to the location of the remaining non-hydrogen atoms, including one and a half (disordered) toluene rings per asymmetric unit. At this point, a second empirical absorption correction[11] was made. All nonsolvent atoms were then anisotropically refined.

Structure Solution and Refinement for $W_2(SePh)Cl_5(dppm) \cdot 3CH_2Cl_2$ (4). The two independent tungsten atoms were located by use of a Patterson map. The systematic absences in the intensity data narrowed the choice of space groups to $Pna2_1$ and $Pnam$. The noncentrosymmetric space group and the first enantiomorph chosen provided the correct solution. All non-hydrogen atoms were located through a series of alternating difference Fourier maps and least-squares refinements. Constraints were placed on all rings, and a low-weight restraint was placed on the Se–C bond distance. While the refinement of the chemical entity $W_2(SePh)Cl_5(dppm)_2$ proceeded routinely, a complex pattern of disordered CH_2Cl_2 molecules made the final stages of the refinement more problematic.

Two dichloromethane molecules were easily found, one at full occupancy, while the other was refined with a multiplicity of 0.46. All of the atoms in the disordered region were located in difference Fourier maps; no a priori chemical modeling was done. The pattern of atomic centers in the disordered region could be interpreted as comprised of as many as five CH_2Cl_2 molecules—all with partial site occupation and some mutually exclusive with others. The model that was refined used these five CH_2Cl_2 moieties. There were three distinct carbon atom sites, two of which were common to two CH_2Cl_2 molecules each. The site occupation factors of all of the atomic sites were functionally connected to a common variable parameter in such a way that (1) the correct chemical stoichiometry for the region was always maintained and (2) the sum of the occupations of any given mutually exclusive pair of CH_2Cl_2 molecules could not exceed 1. In addition, geometrical restraints, in the form of observations, were applied to the C–Cl distances and to the Cl···Cl legs. Thus, geometrical order was imposed with all positional parameters retained as variables. All of the atomic sites attached to a particular carbon center were constrained to a common isotropic displacement parameter.

The parameters for the disordered region were subject to some degree of oscillation; however, the refinement of this region led to chemically acceptable results. Because of the oscillation, three cycles of geometry idealization were carried out. The atoms of this region were included in all structure factor calculations but were not allowed to vary in the final least-squares refinement of the rest of the structure. The final least-squares refinement cycles fit 277 parameters to 3366 observations, including 16 observational restraints.

A total of 2.97 ± 0.07 dichloromethane molecules per tungsten dimer were accounted for. The molecular formula in Table I reflects the average value of three dichloromethane molecules per asymmetric unit. It is not clear that the model employed for the CH_2Cl_2 moieties was the only acceptable one. Indeed, it is not certain that the overall composition of this region remained constant through the course of the intensity data collection. The model refined represents the best fit to the available data. After refinement, several peaks about 1 e/Å^3 remained in the last difference Fourier map. These can be accounted for by incoherent scattering by the solvent molecules in the lattice.

Structure Solution and Refinement for $Mo_2(SPh)Cl_5(dppm)_2 \cdot {}^1/_2CH_2Cl_2 \cdot C_4H_8O \cdot C_6H_6$ (6). A red crystal of **6** was mounted on the end of a glass fiber and secured with epoxy resin. The reduced cell dimensions indicated that the crystal belonged to the monoclinic system; systematic absences led to the choice of $P2_1/n$ as the space group. A Patterson peak search revealed the locations of the two independent Mo

(9) See for example: Bino, A.; Cotton, F. A.; Fanwick, P. E. *Inorg. Chem.* **1979**, *18*, 3558.
(10) North, A. C. T.; Phillips, D. C.; Mathews, F. S. *Acta Crystallogr., Sect. A: Cryst. Phys., Diffr., Theor. Gen. Crystallogr.* **1968**, *A24*, 351.
(11) Walker, N.; Stuart, D. *Acta Crystallogr., Sect. A: Found. Crystallogr.* **1983**, *A39*, 159.

Table II. Atomic Positional Parameters and Equivalent Isotropic Displacement Parameters and Their Estimated Standard Deviations for $W_2(SPh)_2Cl_4(dppm)_2 \cdot 3C_7H_8$[a]

atom	x	y	z	B, Å²
W(1)	0.40998 (3)	0.48187 (3)	0.03703 (3)	3.955 (7)
Cl(1)	0.2331 (2)	0.3916 (2)	−0.0536 (2)	5.69 (6)
Cl(2)	0.3440 (2)	0.5261 (2)	0.2287 (2)	5.67 (5)
S(1)	0.5662 (2)	0.5819 (2)	0.1700 (2)	4.78 (5)
P(1)	0.4714 (2)	0.3088 (2)	0.0528 (2)	4.59 (5)
P(2)	0.3281 (2)	0.6452 (2)	0.0168 (2)	4.45 (5)
C(1)	0.6182 (7)	0.3137 (7)	0.0925 (7)	4.6 (2)
C(2)	0.4312 (8)	0.1852 (7)	−0.0842 (8)	5.1 (2)
C(3)	0.351 (1)	0.1782 (9)	−0.188 (1)	6.8 (3)
C(4)	0.322 (1)	0.081 (1)	−0.286 (1)	7.9 (4)
C(5)	0.375 (1)	−0.005 (1)	−0.280 (1)	8.3 (4)
C(6)	0.461 (1)	0.0020 (9)	−0.178 (1)	7.5 (4)
C(7)	0.488 (1)	0.0989 (8)	−0.075 (1)	6.7 (3)
C(8)	0.4375 (8)	0.2773 (7)	0.1799 (7)	5.2 (2)
C(9)	0.3303 (8)	0.2521 (9)	0.1638 (9)	6.6 (3)
C(10)	0.299 (1)	0.2291 (9)	0.258 (1)	7.5 (3)
C(11)	0.373 (1)	0.2319 (8)	0.3674 (9)	7.2 (3)
C(12)	0.478 (1)	0.2565 (9)	0.382 (1)	7.8 (3)
C(13)	0.5148 (9)	0.2804 (8)	0.2882 (8)	6.2 (3)
C(14)	0.1862 (8)	0.6292 (8)	−0.0558 (9)	5.7 (3)
C(15)	0.1219 (8)	0.6218 (9)	0.022 (1)	6.8 (3)
C(16)	0.0088 (9)	0.6128 (9)	−0.024 (1)	7.7 (3)
C(17)	−0.035 (1)	0.605 (1)	−0.149 (1)	8.5 (4)
C(18)	0.029 (1)	0.615 (1)	−0.222 (1)	10.4 (5)
C(19)	0.142 (1)	0.628 (1)	−0.175 (1)	7.8 (4)
C(20)	0.3372 (8)	0.7670 (7)	0.1560 (8)	5.1 (2)
C(21)	0.2728 (9)	0.8445 (8)	0.136 (1)	6.7 (3)
C(22)	0.278 (1)	0.9388 (9)	0.238 (1)	7.8 (4)
C(23)	0.344 (1)	0.953 (1)	0.357 (1)	7.8 (4)
C(24)	0.408 (1)	0.8748 (9)	0.374 (1)	7.0 (3)
C(25)	0.4029 (8)	0.7783 (8)	0.2726 (8)	5.9 (3)
C(26)	0.6494 (8)	0.5604 (8)	0.3039 (8)	5.5 (2)
C(27)	0.757 (1)	0.595 (1)	0.338 (1)	8.5 (4)
C(28)	0.822 (1)	0.579 (1)	0.443 (1)	10.6 (5)
C(29)	0.776 (1)	0.535 (1)	0.515 (1)	8.8 (4)
C(30)	0.669 (1)	0.5090 (9)	0.4844 (9)	7.1 (3)
C(31)	0.6029 (9)	0.5223 (7)	0.3753 (8)	5.7 (2)
C(32)	−0.001 (2)	0.824 (2)	0.511 (3)	20 (1)*
C(33)	0.081 (2)	0.789 (2)	0.582 (2)	18.0 (9)*
C(34)	0.172 (2)	0.733 (2)	0.520 (3)	19 (1)*
C(35)	0.156 (2)	0.735 (2)	0.408 (3)	20 (1)*
C(36)	0.073 (3)	0.776 (3)	0.347 (4)	27 (2)*
C(37)	−0.011 (3)	0.825 (3)	0.390 (4)	29 (2)*
C(38)	−0.082 (3)	0.883 (3)	0.582 (4)	27 (2)*
C(39)	0.050 (3)	1.033 (3)	0.974 (4)	15 (1)*
C(40)	−0.017 (2)	1.089 (2)	1.036 (2)	15.9 (8)*
C(41)	0.079 (3)	0.937 (3)	0.921 (4)	14 (1)*
C(42)	0.126 (3)	1.019 (3)	0.905 (4)	26 (2)*
C(43)	0.066 (3)	1.110 (3)	0.974 (3)	12 (1)*

[a] Starred values are for atoms refined isotropically. Anisotropically refined atoms are given in the form of the isotropic equivalent thermal parameter defined as $^4/_3[a^2\beta_{11} + b^2\beta_{22} + c^2\beta_{33} + ab(\cos\gamma)\beta_{12} + ac(\cos\beta)\beta_{13} + bc(\cos\alpha)\beta_{23}]$.

atoms. A sequence of successive difference Fourier maps and least-squares cycles led to full development of the coordination sphere. Several molecules of interstitial solvent were also located. These were successfully refined as one benzene and one tetrahydrofuran molecule at full occupancy and a dichloromethane molecule at half-occupancy. Anisotropic refinement was completed to give $R = 0.0666$ and $R_w = 0.0965$ by using 5678 reflections to fit 657 variables.

Final atomic positional and equivalent isotropic thermal parameters for compounds **1**, **4**, and **6** are listed in Tables II–IV, respectively. Selected bond distances and angles are located in Tables V–VII. ORTEP views of the three structurally characterized compounds are shown in Figures 1–3; these define the labeling schemes used in the tables.

Results and Discussion

The choice of $W_2Cl_4(dppm)_2$ and $Mo_2Cl_4(dppm)_2$ for this oxidative-addition study was based on their accessibility as starting materials and on the expectation that the presence of a phosphine bridge with a three-atom backbone (P–C–P) would provide additional stability in both the reaction intermediates and the products in the sense of holding the two metal centers together.

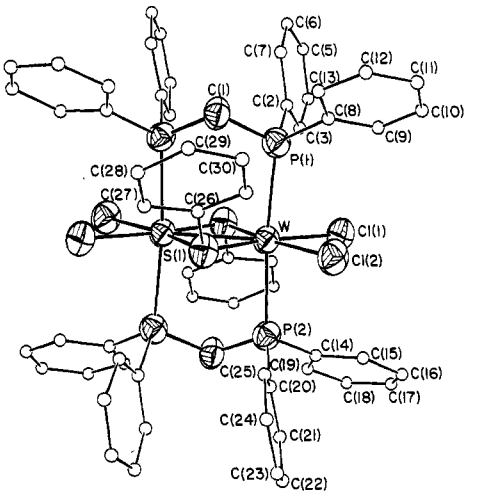

Figure 1. Structure and atom-labeling scheme for $W_2(SPh)_2Cl_4(dppm)_2$ (**1**). With the exception of the carbon atoms of the phenyl rings, the atoms are represented by their 50% probability ellipsoids.

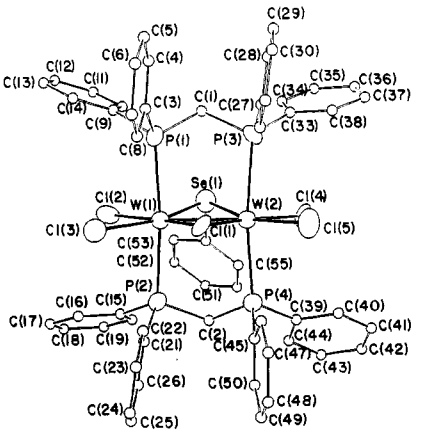

Figure 2. Molecular structure and atom-labeling scheme for $W_2(SePh)Cl_5(dppm)_2$ (**4**).

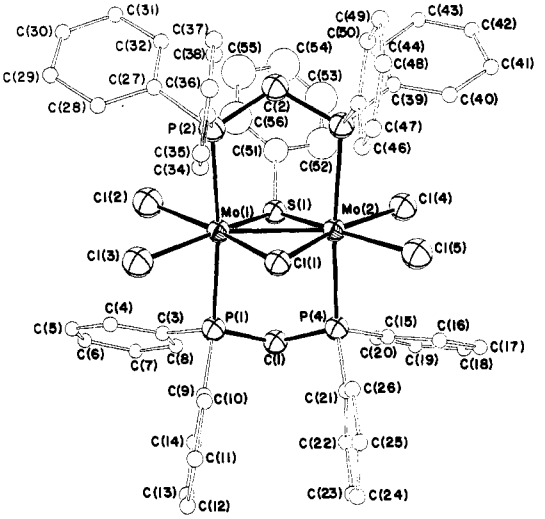

Figure 3. Molecular structure and atom-labeling scheme for $Mo_2(SPh)Cl_5(dppm)_2$ (**6**).

This is especially important with regard to oxidative addition across quadruple bonds since the metal–metal interaction will be weakened significantly by the formation of four additional metal–ligand bonds. Compounds containing bridging phosphines with four-atom backbones (P–C–C–P) are not acceptable due to the strain placed on the molecule from steric requirements, which cause a significant torsion angle down the metal–metal vector. In these compounds, it is unlikely that oxidative addition will occur

Table III. Atomic Positional Parameters and Equivalent Isotropic Displacement Parameters and Their Estimated Standard Deviations for $W_2(SePh)Cl_5(dppm)_2 \cdot 3CH_2Cl_2$[a]

atom	x	y	z	B, Å²	atom	x	y	z	B, Å²
W(1)	0.83369 (4)	0.8977 (1)	1.033	2.45 (4)	C(31)	0.8156 (8)	0.807 (2)	0.514 (2)	5 (1)*
W(2)	0.88735 (4)	0.8528 (1)	0.9009 (2)	2.45 (4)	C(32)	0.8329 (8)	0.805 (2)	0.618 (2)	4 (1)*
Se(1)	0.8737 (1)	0.7765 (3)	1.0838 (4)	3.4 (1)	C(33)	0.8815 (9)	0.628 (2)	0.799 (4)	6 (1)*
Cl(1)	0.8429 (3)	0.9485 (7)	0.8421 (9)	2.4 (3)	C(34)	0.8849 (9)	0.565 (2)	0.884 (4)	4 (1)*
Cl(2)	0.8110 (3)	0.8667 (8)	1.216 (1)	3.9 (3)	C(35)	0.9085 (9)	0.498 (2)	0.871 (4)	15 (3)*
Cl(3)	0.7838 (3)	0.9956 (7)	1.026 (1)	3.7 (3)	C(36)	0.9287 (9)	0.494 (2)	0.773 (4)	7 (2)*
Cl(4)	0.9383 (3)	0.7659 (7)	0.914 (1)	3.3 (3)	C(37)	0.9253 (9)	0.557 (2)	0.689 (4)	19 (4)*
Cl(5)	0.9100 (3)	0.8803 (8)	0.7097 (9)	4.2 (4)	C(38)	0.9017 (9)	0.624 (2)	0.702 (4)	13 (3)*
P(1)	0.7966 (3)	0.7721 (9)	0.956 (1)	3.1 (3)	C(39)	0.9683 (6)	0.962 (2)	0.974 (3)	5 (1)*
P(2)	0.8654 (3)	1.0249 (9)	1.123 (1)	2.9 (3)	C(40)	0.9871 (6)	0.943 (2)	0.877 (3)	3 (1)*
P(3)	0.8572 (3)	0.7200 (7)	0.812 (1)	2.7 (3)	C(41)	1.0221 (6)	0.930 (2)	0.885 (3)	6 (1)*
P(4)	0.9236 (3)	0.9835 (8)	0.966 (1)	2.9 (3)	C(42)	1.0384 (6)	0.936 (2)	0.990 (3)	7 (2)*
C(1)	0.8227 (9)	0.681 (2)	0.914 (4)	2.6 (9)*	C(43)	1.0196 (6)	0.955 (2)	1.087 (3)	8 (2)*
C(2)	0.912 (1)	1.011 (3)	1.105 (3)	2 (1)*	C(44)	0.9845 (6)	0.968 (2)	1.079 (3)	4 (1)*
C(3)	0.7677 (7)	0.792 (2)	0.836 (2)	2.7 (9)*	C(45)	0.9206 (8)	1.084 (2)	0.887 (2)	3.3 (9)*
C(4)	0.7516 (7)	0.723 (2)	0.782 (2)	4 (1)*	C(46)	0.9047 (8)	1.090 (2)	0.781 (2)	1.4 (7)*
C(5)	0.7315 (7)	0.737 (2)	0.687 (2)	6 (1)*	C(47)	0.9068 (8)	1.166 (2)	0.718 (2)	4 (1)*
C(6)	0.7275 (7)	0.821 (2)	0.644 (2)	6 (2)*	C(48)	0.9248 (8)	1.237 (2)	0.760 (2)	5 (1)*
C(7)	0.7436 (7)	0.891 (2)	0.698 (2)	9 (2)*	C(49)	0.9408 (8)	1.232 (2)	0.866 (2)	7 (2)*
C(8)	0.7637 (7)	0.877 (2)	0.793 (2)	5 (1)*	C(50)	0.9387 (8)	1.155 (2)	0.929 (2)	8 (2)*
C(9)	0.7674 (9)	0.719 (2)	1.059 (2)	5 (1)*	C(51)	0.9434 (9)	0.816 (2)	1.405 (2)	9 (2)*
C(10)	0.7818 (9)	0.660 (2)	1.135 (2)	4 (1)*	C(52)	0.9086 (9)	0.800 (2)	1.415 (2)	9 (2)*
C(11)	0.7619 (9)	0.623 (2)	1.220 (2)	7 (1)*	C(53)	0.8885 (9)	0.793 (2)	1.318 (2)	4 (1)*
C(12)	0.7276 (9)	0.645 (2)	1.230 (2)	6 (1)*	C(54)	0.9031 (9)	0.802 (2)	1.210 (2)	6 (1)*
C(13)	0.7132 (9)	0.704 (2)	1.154 (2)	6 (1)*	C(55)	0.9379 (9)	0.817 (2)	1.200 (2)	6 (1)*
C(14)	0.7331 (9)	0.741 (2)	1.069 (2)	7 (2)*	C(56)	0.9580 (9)	0.825 (2)	1.297 (2)	7 (2)*
C(15)	0.8578 (7)	1.033 (2)	1.276 (2)	1.7 (8)*	C(60)	0.731 (2)	−0.087 (5)	0.271 (6)	11 (2)*
C(16)	0.8273 (7)	1.071 (2)	1.309 (2)	6 (1)*	Cl(10)	0.7332 (6)	−0.026 (1)	0.401 (2)	13.0 (6)*
C(17)	0.8190 (7)	1.077 (2)	1.424 (2)	7 (1)*	Cl(20)	0.6858 (6)	−0.075 (1)	0.233 (2)	12.6 (7)*
C(18)	0.8412 (7)	1.044 (2)	1.506 (2)	5 (1)*	C(70)	−0.024 (3)	0.636 (3)	0.16 (1)	15*
C(19)	0.8717 (7)	1.005 (2)	1.472 (2)	4 (1)*	Cl(30)	0.010 (1)	0.620 (3)	0.064 (4)	15*
C(20)	0.8800 (7)	1.000 (2)	1.358 (2)	6 (1)*	Cl(40)	−0.038 (1)	0.535 (4)	0.209 (5)	15*
C(21)	0.8585 (8)	1.136 (1)	1.074 (2)	3 (1)*	C(80)	0.524 (5)	0.740 (3)	0.72 (1)	19*
C(22)	0.8415 (8)	1.156 (1)	0.973 (2)	3 (1)*	Cl(50)	0.544 (2)	0.808 (4)	0.821 (4)	19*
C(23)	0.8399 (8)	1.241 (1)	0.934 (2)	4 (1)*	Cl(60)	0.504 (2)	0.806 (4)	0.620 (4)	19*
C(24)	0.8552 (8)	1.308 (1)	0.997 (2)	3 (1)*	C(90)	0.630 (2)	0.917 (3)	0.963 (3)	19*
C(25)	0.8722 (8)	1.288 (1)	1.097 (2)	5 (1)*	Cl(80)	0.608 (1)	0.823 (3)	0.919 (6)	19*
C(26)	0.8738 (8)	1.203 (1)	1.136 (2)	5 (1)*	Cl(95)	0.636 (1)	0.986 (2)	0.846 (3)	19*
C(27)	0.8370 (8)	0.726 (2)	0.675 (2)	4 (1)*	Cl(96)	0.6699 (9)	0.921 (3)	0.896 (5)	19*
C(28)	0.8239 (8)	0.649 (2)	0.629 (2)	4 (1)*	C(100)	0.6699 (9)	0.921 (3)	0.896 (5)	19*
C(29)	0.8067 (8)	0.652 (2)	0.525 (2)	6 (1)*	Cl(70)	0.674 (3)	0.828 (5)	0.809 (9)	19*
C(30)	0.8026 (8)	0.730 (2)	0.468 (2)	6 (1)*	Cl(90)	0.653 (2)	0.822 (4)	0.948 (9)	19*

[a] Starred values are for atoms refined isotropically. Anisotropically refined atoms are given in the form of the isotropic equivalent displacement parameter defined as $^4/_3[a^2\beta_{11} + b^2\beta_{22} + c^2\beta_{33} + ab(\cos\gamma)\beta_{12} + ac(\cos\beta)\beta_{13} + bc(\cos\alpha)\beta_{23}]$.

without either rearrangement of the bridging ligands into chelating ligands or disruption of the metal–metal bond to give monomers. In the reaction of β-$Mo_2Cl_4(dppe)_2$ with chlorine and of β-$Mo_2Cl_4(dto)_2$ with EtSSEt, the products are α-$Mo_2Cl_6(dppe)_2$ and α-$Mo_2(SEt)_2Cl_4(dto)_2$,[4,10] respectively. Avoidance of this problem in the oxidative addition of β-$W_2Cl_4(dppm)_2$ and β-$Mo_2Cl_4(dmpm)_2$ with chlorine to give $W_2Cl_6(dppm)_2$ and $Mo_2Cl_6(dmpm)_2$, respectively,[3a] provided guidance in selecting the reactions reported here, which are summarized in Scheme I.

When this work was begun, we did not foresee that the W_2^{4+} core would be so easily oxidized by CH_2Cl_2 and therefore chose this as the solvent in the first experiments. When we became aware that it was a reactant as well as a solvent, we carried out reactions in toluene and found that the chemistry is then simpler. The reaction of $W_2Cl_4(dppm)_2$ with PhSSPh in toluene produces a cherry red solution from which the only characterized product is $W_2(SPh)_2Cl_4(dppm)_2$ (**1**). If dichloromethane is used as the solvent, a mixture of two products is obtained, namely, $W_2(SPh)Cl_5(dppm)_2$ (**2**) and $W_2Cl_6(dppm)_2$ (**5**). Whether **1** is an intermediate in this reaction could not be determined by monitoring the visible spectrum of the reaction mixture because of overlapping of the electronic absorption bands of $W_2Cl_4(dppm)_2$ (in toluene: 496, 738 nm) and **1** (in toluene: 504, 730 nm). The reaction of **1** with dichloromethane could be followed by visible spectroscopy. As in the previous reaction, both **2** and **5** are formed. Three of the spectra from this reaction are shown in Figure 4. The proximity of the absorption bands for **1** (in toluene: 504, 730 nm), (in CH_2Cl_2: 435 nm), and **5** (in CH_2Cl_2: 465, 384 nm) complicate these spectra to the extent that in most cases one observes in the early reaction stage only one broad absorption band, which shifts as the reaction progresses. The initial spectrum (solid line) was taken approximately 15 min after the commencement of the reaction and shows a major absorption at 490 nm, which

Scheme I

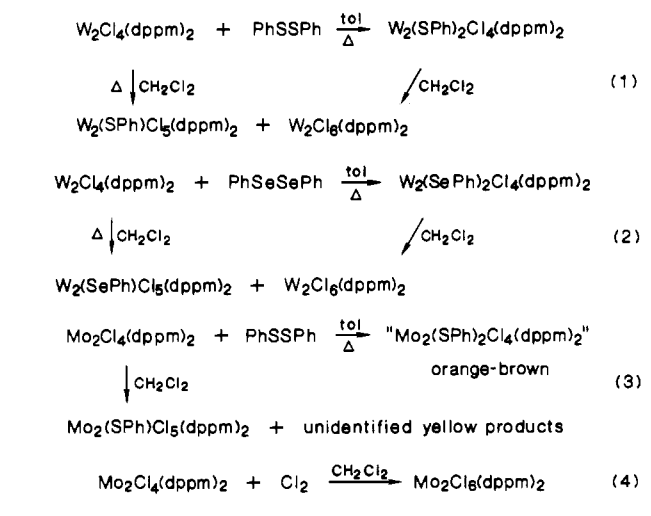

Table IV. Atomic Positional Parameters and Equivalent Isotropic Displacement Parameters and Their Estimated Standard Deviations for $Mo_2(SPh)Cl_5(dppm)_2 \cdot {}^1/_2CH_2Cl_2 \cdot OC_4H_8 \cdot C_6H_6$[a]

atom	x	y	z	B, Å²	atom	x	y	z	B, Å²
Mo(1)	0.47940 (7)	0.24141 (4)	0.19426 (4)	2.47 (2)	C(30)	0.417 (1)	0.0162 (6)	0.2978 (7)	6.7 (4)
Mo(2)	0.35083 (7)	0.33517 (4)	0.19963 (4)	2.41 (2)	C(31)	0.316 (1)	0.0447 (6)	0.2974 (7)	7.2 (4)
Cl(1)	0.5463 (2)	0.3247 (1)	0.2434 (1)	3.03 (5)	C(32)	0.322 (1)	0.1024 (6)	0.2977 (7)	7.0 (4)
Cl(2)	0.4524 (3)	0.1497 (1)	0.1580 (1)	4.50 (7)	C(33)	0.5246 (9)	0.2199 (5)	0.3611 (5)	3.9 (3)
Cl(3)	0.6742 (2)	0.2103 (1)	0.2249 (1)	4.08 (7)	C(34)	0.629 (1)	0.2481 (5)	0.3615 (6)	5.0 (3)
Cl(4)	0.1620 (2)	0.3674 (1)	0.1637 (1)	3.90 (6)	C(35)	0.693 (1)	0.2621 (7)	0.4148 (6)	6.3 (4)
Cl(5)	0.3717 (2)	0.4266 (1)	0.2423 (1)	4.12 (6)	C(36)	0.656 (1)	0.2506 (7)	0.4685 (6)	6.6 (4)
S(1)	0.2925 (2)	0.2563 (1)	0.1411 (1)	2.91 (5)	C(37)	0.555 (1)	0.2216 (7)	0.4665 (6)	6.6 (4)
P(1)	0.5409 (2)	0.2709 (1)	0.0973 (1)	2.80 (6)	C(38)	0.489 (1)	0.2066 (6)	0.4127 (5)	5.2 (3)
P(2)	0.4331 (2)	0.2035 (1)	0.2912 (1)	2.97 (6)	C(39)	0.1337 (9)	0.3164 (5)	0.2921 (4)	3.8 (3)
P(3)	0.2824 (2)	0.3027 (1)	0.2933 (1)	2.95 (6)	C(40)	0.107 (1)	0.3724 (6)	0.3012 (6)	5.5 (3)
P(4)	0.4044 (2)	0.3741 (1)	0.1052 (1)	2.81 (6)	C(41)	−0.008 (1)	0.3857 (7)	0.2997 (6)	5.8 (3)
C(1)	0.4379 (8)	0.3190 (5)	0.0568 (4)	3.1 (2)	C(42)	−0.092 (1)	0.3439 (7)	0.2900 (6)	5.8 (4)
C(2)	0.2922 (8)	0.2282 (4)	0.3004 (4)	3.2 (2)	C(43)	−0.066 (1)	0.2911 (7)	0.2808 (6)	5.6 (4)
C(3)	0.5433 (8)	0.2146 (5)	0.0466 (4)	3.5 (2)	C(44)	0.0523 (9)	0.2773 (6)	0.2816 (5)	4.7 (3)
C(4)	0.6130 (9)	0.1699 (5)	0.0648 (5)	4.4 (3)	C(45)	0.3465 (9)	0.3277 (5)	0.3650 (5)	4.0 (3)
C(5)	0.623 (1)	0.1273 (6)	0.0288 (6)	5.7 (3)	C(46)	0.443 (1)	0.3581 (5)	0.3745 (5)	4.6 (3)
C(6)	0.565 (1)	0.1267 (6)	−0.0263 (7)	6.3 (4)	C(47)	0.495 (1)	0.3731 (7)	0.4317 (7)	6.6 (4)
C(7)	0.492 (1)	0.1707 (8)	−0.0483 (7)	7.5 (4)	C(48)	0.448 (1)	0.3588 (7)	0.4785 (6)	6.9 (4)
C(8)	0.479 (1)	0.2154 (6)	−0.0107 (5)	5.4 (3)	C(49)	0.346 (1)	0.3267 (7)	0.4698 (6)	5.9 (4)
C(9)	0.6749 (8)	0.3055 (5)	0.0935 (5)	3.4 (2)	C(50)	0.2984 (9)	0.3119 (6)	0.4138 (5)	5.0 (3)
C(10)	0.7485 (8)	0.3240 (5)	0.1432 (5)	3.6 (3)	C(51)	0.1708 (8)	0.2157 (5)	0.1502 (4)	3.6 (2)
C(11)	0.848 (1)	0.3495 (6)	0.1365 (5)	5.0 (3)	C(52)	0.0658 (9)	0.2445 (6)	0.1327 (6)	5.2 (3)
C(12)	0.876 (1)	0.3573 (6)	0.0831 (6)	5.3 (3)	C(53)	−0.027 (1)	0.2135 (6)	0.1376 (7)	6.4 (4)
C(13)	0.799 (1)	0.3368 (6)	0.0317 (5)	5.6 (3)	C(54)	−0.029 (1)	0.1610 (7)	0.1533 (7)	6.9 (4)
C(14)	0.7025 (9)	0.3120 (6)	0.0371 (5)	4.8 (3)	C(55)	0.079 (1)	0.1343 (7)	0.1718 (8)	7.7 (4)
C(15)	0.2925 (9)	0.4114 (5)	0.0590 (5)	3.7 (3)	C(56)	0.182 (1)	0.1646 (6)	0.1706 (7)	6.0 (4)
C(16)	0.268 (1)	0.4631 (5)	0.0792 (5)	5.1 (3)	C(57)	0.6463	0.0008	−0.0891	9*
C(17)	0.179 (1)	0.4939 (6)	0.0445 (6)	5.7 (3)	Cl(6)	0.7505	−0.0019	−0.1158	18*
C(18)	0.124 (1)	0.4740 (7)	−0.0086 (6)	6.1 (3)	Cl(7)	0.7346	−0.0391	−0.0325	18*
C(19)	0.150 (1)	0.4229 (7)	−0.0286 (6)	6.3 (4)	O(1)	0.484 (1)	0.3584 (8)	0.9212 (8)	13.3 (5)*
C(20)	0.2337 (9)	0.3917 (6)	0.0060 (5)	4.5 (3)	C(58)	0.417 (2)	0.371 (1)	0.824 (1)	11.0 (6)*
C(21)	0.5252 (8)	0.4206 (4)	0.1111 (5)	3.1 (2)	C(59)	0.398 (2)	0.346 (1)	0.877 (1)	14.2 (8)*
C(22)	0.5510 (9)	0.4405 (5)	0.0581 (5)	4.5 (3)	C(60)	0.578 (2)	0.388 (1)	0.898 (1)	14.7 (9)*
C(23)	0.643 (1)	0.4756 (7)	0.0608 (6)	6.4 (4)	C(61)	0.523 (2)	0.400 (1)	0.838 (1)	11.8 (7)*
C(24)	0.708 (1)	0.4914 (6)	0.1136 (6)	5.7 (3)	C(62)	0.743 (2)	0.4494 (9)	0.3654 (9)	9.8 (5)*
C(25)	0.678 (1)	0.4716 (6)	0.1652 (6)	5.1 (3)	C(63)	0.648 (2)	0.473 (1)	0.3310 (9)	10.1 (5)*
C(26)	0.5846 (9)	0.4367 (5)	0.1631 (5)	3.8 (3)	C(64)	0.648 (1)	0.5252 (9)	0.3079 (8)	9.2 (5)*
C(27)	0.4245 (9)	0.1296 (5)	0.2963 (5)	3.9 (3)	C(65)	0.757 (1)	0.5514 (8)	0.3154 (8)	8.4 (5)*
C(28)	0.522 (1)	0.0995 (5)	0.2953 (6)	5.3 (3)	C(66)	0.844 (1)	0.5320 (9)	0.3471 (8)	8.9 (5)*
C(29)	0.520 (1)	0.0413 (6)	0.2966 (7)	6.7 (4)	C(67)	0.843 (2)	0.484 (1)	0.376 (1)	12.3 (7)*

[a] Starred values are for atoms refined isotropically. Anisotropically refined atoms are given in the form of the isotropic equivalent displacement parameter defined as $^4/_3[a^2\beta_{11} + b^2\beta_{22} + c^2\beta_{33} + ab(\cos\gamma)\beta_{12} + ac(\cos\beta)\beta_{13} + bc(\cos\alpha)\beta_{23}]$.

Table V. Selected Bond Distances (Å) and Bond Angles (deg) and Their Estimated Standard Deviations for $W_2(SPh)_2Cl_4(dppm)_2$ (**1**)

W(1)′–W(1)	2.787 (1)	S(1)–C(26)	1.803 (10)
W(1)–Cl(1)	2.443 (2)	P(1)–C(1)	1.852 (9)
W(1)–Cl(2)	2.452 (2)	P(1)–C(2)	1.849 (8)
W(1)–S(1)	2.350 (2)	P(1)–C(8)	1.837 (11)
W(1)–S(1)′	2.350 (2)	P(2)–C(1)′	1.844 (11)
W(1)–P(1)	2.570 (3)	P(2)–C(14)	1.821 (10)
W(1)–P(2)	2.548 (3)	P(2)–C(20)	1.853 (8)
W(1)′–W(1)–Cl(1)	140.29 (6)	S(1)–W(1)–P(1)	95.63 (8)
W(1)′–W(1)–Cl(2)	139.89 (5)	S(1)–W(1)–P(2)	90.04 (8)
W(1)′–W(1)–S(1)	53.63 (6)	S(1)–W(1)–P(1)	87.34 (8)
W(1)′–W(1)–S(1)′	53.62 (6)	S(1)′–W(1)–P(2)	93.78 (8)
W(1)′–W(1)–P(1)	92.49 (6)	P(1)–W(1)–P(2)	173.62 (8)
W(1)′–W(1)–P(2)	93.22 (6)	W(1)–S(1)–W(1)′	72.75 (5)
Cl(1)–W(1)–Cl(2)	79.81 (8)	W(1)–S(1)–C(26)	125.9 (4)
Cl(1)–W(1)–S(1)	166.06 (8)	W(1)′–S(1)–C(26)	125.8 (3)
Cl(1)–W(1)–S(1)′	86.67 (8)	W(1)–P(1)–C(1)	109.6 (3)
Cl(1)–W(1)–P(1)	85.44 (8)	W(1)–P(1)–C(2)	120.7 (3)
Cl(1)–W(1)–P(2)	88.36 (8)	W(1)–P(1)–C(8)	115.7 (3)
Cl(2)–W(1)–S(1)	86.26 (7)	W(1)–P(2)–C(1)′	111.0 (3)
Cl(2)–W(1)–S(1)′	166.48 (8)	W(1)–P(2)–C(14)	115.0 (4)
Cl(2)–W(1)–P(1)	91.51 (8)	W(1)–P(2)–C(20)	121.9 (3)
Cl(2)–W(1)–P(2)	85.94 (8)	P(1)–C(1)–P(2)′	111.0 (5)
S(1)–W(1)–S(1)′	107.25 (8)		

is primarily due to **1**. The dashed-line spectrum represents the reaction 45 min later. The peak at 490 nm has now shifted to 470 nm, indicating a decrease in concentration of **1** and an increase in the formation of **2** and **5**. The third spectrum (dotted line), taken 30 h later, is typical for the reaction mixture between 1 and 3 days later. The separation between the bands for **2** (435 nm) and **5** (465 nm) can clearly be seen. The actual maximum absorption occurs at 455 nm with the peak center at 450 nm.

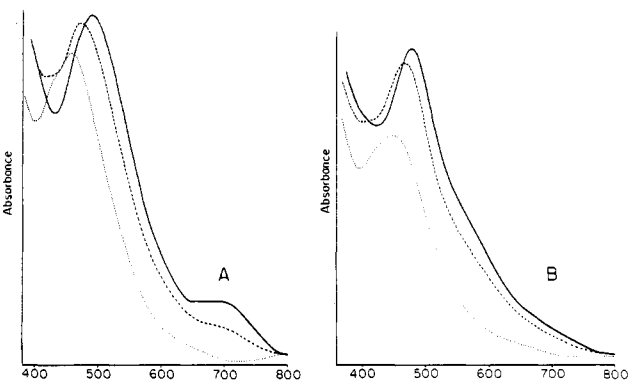

Figure 4. Electronic absorption spectra of products in the reactions between $W_2(SPh)_2Cl_4(dppm)_2$ and CH_2Cl_2 (A) and $W_2(SePh)_2Cl_4(dppm)_2$ and CH_2Cl_2 (B).

The oxidative-addition chemistry of $W_2Cl_4(dppm)_2$ with PhSeSePh behaves analogously to the PhSSPh chemistry. When the reaction is carried out in toluene, a purple solution of $W_2(SePh)_2Cl_4(dppm)_2$ (**3**) is cleanly produced. When dichloromethane is used as the solvent, a mixture of $W_2(SePh)Cl_5(dppm)_2$ (**4**) and $W_2Cl_6(dppm)_2$ (**5**) is produced. Once again, the over-

Table VI. Selected Bond Distances (Å) and Bond Angles (deg) and Their Estimated Standard Deviations for $W_2(SePh)Cl_5(dppm)_2$ (**4**)

W(1)–W(2)	2.708 (2)	W(2)–Cl(4)	2.413 (10)	P(2)–C(15)	1.83 (2)
W(1)–Se(1)	2.513 (5)	W(2)–Cl(5)	2.457 (11)	P(2)–C(21)	1.83 (3)
W(1)–Cl(1)	2.401 (10)	W(2)–P(3)	2.584 (12)	P(3)–C(1)	1.91 (4)
W(1)–Cl(2)	2.388 (12)	W(2)–P(4)	2.578 (13)	P(3)–C(27)	1.80 (3)
W(1)–Cl(3)	2.474 (11)	Se(1)–C(54)	1.93 (3)	P(3)–C(33)	1.71 (3)
W(1)–P(1)	2.583 (13)	P(1)–C(1)	1.80 (4)	P(4)–C(2)	1.76 (4)
W(1)–P(2)	2.553 (13)	P(1)–C(3)	1.84 (3)	P(4)–C(39)	1.79 (3)
W(2)–Se(1)	2.509 (5)	P(1)–C(9)	1.86 (3)	P(4)–C(45)	1.81 (3)
W(2)–Cl(1)	2.388 (11)	P(2)–C(2)	1.86 (4)		
W(2)–W(1)–Se(1)	57.3 (1)	P(1)–W(1)–P(2)	174.1 (4)	Cl(5)–W(2)–P(4)	86.3 (4)
W(2)–W(1)–Cl(1)	55.4 (3)	W(1)–W(2)–Se(1)	57.4 (1)	P(3)–W(2)–P(4)	171.7 (4)
W(2)–W(1)–Cl(2)	139.4 (3)	W(1)–W(2)–Cl(1)	55.8 (3)	W(1)–Se(1)–W(2)	65.3 (1)
W(2)–W(1)–Cl(3)	139.1 (3)	W(1)–W(2)–Cl(4)	138.7 (3)	W(1)–Se(1)–C(54)	114. (1)
W(2)–W(1)–P(1)	92.8 (3)	W(1)–W(2)–Cl(5)	139.7 (3)	W(2)–Se(1)–C(54)	116. (1)
W(2)–W(1)–P(2)	93.0 (3)	W(1)–W(2)–P(3)	94.4 (3)	W(1)–Cl(1)–W(2)	68.9 (3)
Se(1)–W(1)–Cl(1)	111.8 (3)	W(1)–W(2)–P(4)	93.6 (3)	W(1)–P(1)–C(1)	111 (1)
Se(1)–W(1)–Cl(2)	82.5 (3)	Se(1)–W(2)–Cl(1)	112.3 (3)	W(1)–P(1)–C(3)	119 (1)
Se(1)–W(1)–Cl(3)	162.8 (3)	Se(1)–W(2)–Cl(4)	82.1 (3)	W(1)–P(1)–C(9)	116 (1)
Se(1)–W(1)–P(1)	83.4 (3)	Se(1)–W(2)–Cl(5)	160.7 (3)	W(1)–P(2)–C(2)	110 (1)
Se(1)–W(1)–P(2)	99.3 (3)	Se(1)–W(2)–P(3)	83.2 (3)	W(1)–P(2)–C(15)	112 (1)
Cl(1)–W(1)–Cl(2)	165.1 (4)	Se(1)–W(2)–P(4)	103.2 (3)	W(1)–P(2)–C(21)	121 (1)
Cl(1)–W(1)–Cl(3)	83.9 (4)	Cl(1)–W(2)–Cl(4)	165.5 (4)	W(2)–P(3)–C(1)	108 (1)
Cl(1)–W(1)–P(1)	90.0 (4)	Cl(1)–W(2)–Cl(5)	83.9 (4)	W(2)–P(3)–C(27)	122 (1)
Cl(1)–W(1)–P(2)	93.9 (4)	Cl(1)–W(2)–P(3)	91.8 (4)	W(2)–P(3)–C(33)	116 (1)
Cl(2)–W(1)–Cl(3)	81.5 (4)	Cl(1)–W(2)–P(4)	90.6 (4)	W(2)–P(4)–C(2)	109 (1)
Cl(2)–W(1)–P(1)	87.5 (4)	Cl(4)–W(2)–Cl(5)	81.6 (4)	W(2)–P(4)–C(39)	114 (1)
Cl(2)–W(1)–P(2)	87.6 (4)	Cl(4)–W(2)–P(3)	88.3 (4)	W(2)–P(4)–C(45)	119 (1)
Cl(3)–W(1)–P(1)	89.8 (4)	Cl(4)–W(2)–P(4)	87.3 (4)	P(1)–C(1)–P(3)	109 (2)
Cl(3)–W(1)–P(2)	86.2 (4)	Cl(5)–W(2)–P(3)	86.0 (4)	P(2)–C(2)–P(4)	113 (2)

Table VII. Selected Bond Distances (Å) and Bond Angles (deg) and Their Estimated Standard Deviations for $Mo_2(SPh)Cl_5(dppm)_2$ (**6**)

Mo(1)–Mo(2)	2.788 (1)	Mo(2)–Cl(5)	2.443 (3)	P(2)–C(27)	1.82 (1)
Mo(1)–Cl(1)	2.405 (3)	Mo(2)–S(1)	2.394 (3)	P(2)–C(33)	1.84 (1)
Mo(1)–Cl(2)	2.399 (3)	Mo(2)–P(3)	2.602 (3)	P(3)–C(2)	1.83 (1)
Mo(1)–Cl(3)	2.453 (3)	Mo(2)–P(4)	2.591 (3)	P(3)–C(39)	1.82 (1)
Mo(1)–S(1)	2.395 (2)	S(1)–C(51)	1.82 (1)	P(3)–C(45)	1.81 (1)
Mo(1)–P(1)	2.611 (3)	P(1)–C(1)	1.84 (1)	P(4)–C(1)	1.85 (1)
Mo(1)–P(2)	2.599 (3)	P(1)–C(3)	1.82 (1)	P(4)–C(15)	1.81 (1)
Mo(2)–Cl(1)	2.408 (2)	P(1)–C(9)	1.85 (1)	P(4)–C(21)	1.84 (1)
Mo(2)–Cl(4)	2.414 (3)	P(2)–C(2)	1.86 (1)		
Mo(2)–Mo(1)–Cl(1)	54.66 (6)	P(1)–Mo(1)–P(2)	173.94 (9)	S(1)–Mo(2)–P(4)	84.53 (9)
Mo(2)–Mo(1)–Cl(2)	138.18 (8)	Mo(1)–Mo(2)–Cl(1)	54.55 (7)	P(3)–Mo(2)–P(4)	174.78 (9)
Mo(2)–Mo(1)–Cl(3)	139.11 (8)	Mo(1)–Mo(2)–Cl(4)	138.82 (8)	Mo(1)–Cl(1)–Mo(2)	70.79 (7)
Mo(2)–Mo(1)–S(1)	54.37 (7)	Mo(1)–Mo(2)–Cl(5)	139.11 (7)	Mo(1)–S(1)–Mo(2)	71.20 (7)
Mo(2)–Mo(1)–P(1)	93.58 (7)	Mo(1)–Mo(2)–S(1)	54.43 (6)	Mo(1)–S(1)–C(51)	124.2 (3)
Mo(2)–Mo(1)–P(2)	92.42 (7)	Mo(1)–Mo(2)–P(3)	93.07 (7)	Mo(2)–S(1)–C(51)	122.1 (4)
Cl(1)–Mo(1)–Cl(2)	166.68 (9)	Mo(1)–Mo(2)–P(4)	91.96 (7)	Mo(1)–P(1)–C(1)	110.3 (4)
Cl(1)–Mo(1)–Cl(3)	84.51 (9)	Cl(1)–Mo(2)–Cl(4)	166.6 (1)	Mo(1)–P(1)–C(3)	113.3 (4)
Cl(1)–Mo(1)–S(1)	108.61 (9)	Cl(1)–Mo(2)–Cl(5)	84.57 (9)	Mo(1)–P(1)–C(9)	124.3 (3)
Cl(1)–Mo(1)–P(1)	93.07 (9)	Cl(1)–Mo(2)–S(1)	108.56 (9)	Mo(1)–P(2)–C(2)	109.6 (3)
Cl(1)–Mo(1)–P(2)	89.76 (9)	Cl(1)–Mo(2)–P(3)	93.00 (9)	Mo(1)–P(2)–C(27)	115.9 (4)
Cl(2)–Mo(1)–Cl(3)	82.7 (1)	Cl(1)–Mo(2)–P(4)	91.04 (9)	Mo(1)–P(2)–C(33)	120.2 (4)
Cl(2)–Mo(1)–S(1)	84.6 (1)	Cl(4)–Mo(2)–Cl(5)	82.1 (1)	Mo(2)–P(3)–C(2)	110.8 (4)
Cl(2)–Mo(1)–P(1)	89.7 (1)	Cl(4)–Mo(2)–S(1)	84.58 (9)	Mo(2)–P(3)–C(39)	113.4 (4)
Cl(2)–Mo(1)–P(2)	86.3 (1)	Cl(4)–Mo(2)–P(3)	87.9 (1)	Mo(2)–P(3)–C(45)	121.5 (4)
Cl(3)–Mo(1)–S(1)	163.9 (1)	Cl(4)–Mo(2)–P(4)	87.4 (1)	Mo(2)–P(4)–C(1)	111.6 (4)
Cl(3)–Mo(1)–P(1)	85.71 (9)	Cl(5)–Mo(2)–S(1)	165.51 (9)	Mo(2)–P(4)–C(15)	114.4 (4)
Cl(3)–Mo(1)–P(2)	89.2 (1)	Cl(5)–Mo(2)–P(3)	87.9 (1)	Mo(2)–P(4)–C(21)	119.0 (3)
S(1)–Mo(1)–P(1)	84.41 (9)	Cl(5)–Mo(2)–P(4)	89.2 (1)	P(1)–C(1)–P(4)	110.9 (5)
S(1)–Mo(1)–P(2)	99.76 (9)	S(1)–Mo(2)–P(3)	97.3 (1)	P(2)–C(2)–P(3)	111.0 (6)

lapping regions in the visible spectra of $W_2Cl_4(dppm)_2$ and the possible reaction intermediate, **3**, precluded a determination of whether this species was present in the reaction mixture. Lastly, the reaction of **3** with dichloromethane was followed spectroscopically. Figure 4 also contains three spectra at various time intervals during the course of this reaction. The spectrum taken 30 min into the course of the reaction (solid line) shows a maximum at 480 nm that is indicative of a mixture of **3**, **4**, and **5**. In the spectrum taken $^1/_2$ h later (dashed line), the absorption band was shifted to 470 nm, indicating a decrease in **3** and, correspondingly, an increase in product formation. After 35 h the maximum had shifted further to higher energies and a distinct separation could be seen between the absorptions from **4** (430 nm) and **5** (465 nm). The absorption band is actually centered at 445 nm with its maximum at 450 nm.

While both **1** and **3** are air-stable solids, their toluene solutions are air-sensitive. The solutions are also somewhat unstable thermally and begin to decompose when heated at higher temperatures (e.g., with refluxing toluene) or during longer reaction times (>30 min). Thus, very mild reaction conditions are necessary to obtain reasonable product yields. Fortunately, this could be accomplished because of the relative ease of oxidizing $W_2Cl_4(dppm)_2$. This, however, presents a problem in regard to oxidative-addition reactions of $Mo_2Cl_4(dppm)_2$ with diphenyl disulfide.

The quadruple bond of $Mo_2Cl_4(dppm)_2$ is much less susceptible to oxidative addition than the ditungsten analogue as evidenced by the sluggish nature of the reaction of the Mo_2 compound with

Table VIII. Selected Bond Distances (Å) and Angles (deg) for $W_2(SPh)_2Cl_4(dppm)_2$ (**1**), $W_2(SePh)Cl_5(dppm)_2$ (**4**), $W_2Cl_6(dppm)_2$ (**5**), $Mo_2(SPh)Cl_5(dppm)_2$ (**6**), and $Mo_2Cl_6(dppm)_2$ (**7**)[a]

compd	1	4	5	6	7
M–M	2.787 (1)	2.708 (2)	2.691 (1)	2.788 (1)	2.789 (1)
M–Cl_{br}		2.395 [7]	2.399 [6]	2.407 [2]	2.403 [1]
M–E[b]	2.350 [0]	2.511 [2]		2.395 [1]	
M–Cl_t	2.448 [5]	2.401 [13]	2.412 [2]	2.407 [8]	2.397 [4]
		2.466 [9]		2.448 [5]	
M–P	2.575 [5]	2.575 [7]	2.564 [3]	2.601 [4]	2.586 [1]
M–Cl_{br}–M		68.9 (3)	68.23 (9)	70.79 (7)	70.92 (5)
M–E–M	72.75 (5)	65.3 (2)		71.20 (7)	
Cl_{br}–M–Cl_{br}			111.77 (9)		109.08 (5)
E–M–E′	107.25 (8)				
Cl_{br}–M–E		112.1 [3]		108.59 [3]	
Cl_t–M–Cl_t	79.81 (8)	81.6 [1]	84.1 (1)	82.4 [3]	84.55 (8)
P–M–P	173.62 (8)	172.9 [12]	172.6 (1)	174.4 [4]	174.41 (7)

[a] Numbers in parentheses are estimated standard deviations. Numbers in brackets are calculated from the equation $[\sum\Delta_i^2/n(n-1)]^{0.5}$, where Δ_i is the deviation of the ith value from the arithmetic mean and n is the total number of values averaged. [b] E = S for compounds **1** and **6** and Se for compound **4**.

PhSSPh. At room temperature in CH_2Cl_2, the reaction proceeds very slowly to give several products, one of which is $Mo_2(SPh)Cl_5(dppm)_2$ (**6**). No reaction is observed in toluene at room temperature, but under reflux conditions an orange-brown product is formed. The compound has not been fully characterized, but we believe it is the logical product $Mo_2(SPh)_2Cl_4(dppm)_2$ by analogy to the ditungsten chemistry that produced $W_2(SPh)_2Cl_4(dppm)_2$ (**1**). The IR spectral properties of the two compounds are very similar (vide supra).

Strong oxidizing agents such as halogens react quickly with $Mo_2Cl_4(dppm)_2$ at room temperature to give $Mo_2X_6(dppm)_2$ compounds. The reaction with Cl_2 produces $Mo_2Cl_6(dppm)_2$ in high yield. Previously, this molecule was reported as a very low yield product from the reaction between $K_4Mo_2Cl_8$ and $(Ph_2P)_3CH$[3b] and in bulk from the melt reaction of $MoCl_3(THF)_3$ and dppm.[8] The compound is very insoluble when prepared by the latter procedure, whereas the oxidative-addition route leads to a reasonably soluble form of the complex. Additional reactions of halogens with $Mo_2X_4(dppm)_2$ (X = Cl, Br, I) compounds have been investigated and will be reported elsewhere.[12]

Structural Results. All compounds with the exception of $W_2(SePh)_2Cl_4(dppm)_2$ (**3**) have been fully or partially structurally characterized. From the analogous preparation and reaction chemistry of $W_2(SPh)_2Cl_4(dppm)_2$ (**1**), compound **3** can be presumed to be structurally similar. A data set was obtained for $W_2(SPh)Cl_5(dppm)_2$ (**2**), which showed the same general geometrical features found in $W_2(SePh)Cl_5(dppm)_2$ (**4**). The structure is not reported here because of problems with refinement. The unit cell parameters for the compound, which contained one $W_2(SPh)Cl_5(dppm)_2$ (**2**) molecule and two toluene molecules per asymmetric unit, were measured: a = 17.834 (4) Å, b = 11.665 (3) Å, c = 32.392 (8) Å, β = 98.81 (2)°, V = 6659 (5) Å^3, Z = 4, W–W = 2.810 (5) Å. The structures of compounds $W_2Cl_6(dppm)_2$ (**5**) and $Mo_2Cl_6(dppm)_2$ (**7**) have been previously reported.[3a,b] Tables V–VII contain selected bond distances and angles for compounds **1**, **4**, and **6**, respectively. Complete lists of molecular dimensions for these compounds are available as supplementary material. Table VIII contains average bond distances and angles for compounds **1**, **4**, and **6** and, for comparison, those parameters previously reported for compounds **5** and **7**.

The dimeric species reported here were produced via the oxidation of the M_2^{4+} core (quadruply bonded) to the M_2^{6+} core. All structurally characterized compounds crystallized as edge-sharing bioctahedra containing trans-bridging bidentate phosphines and four chlorine atoms in equatorial positions. The differentiating features among these compounds are the bridging ligands. Compound **1** contains two bridging chalcogen (SPh) ligands, compounds **4** and **6** contain one bridging chalcogen ligand, either SPh (**6**) or SePh (**4**), and compounds **5** and **7** contain two bridging chlorine ligands. General structural trends include increasing Cl_t–W–Cl_t bond angles with decreasing metal–metal bond length and increasing P–M–P bond angles with increasing metal–metal bond length. Also, with increasing metal–metal bond distance the W–Cl_{br} bond distance increases as do the W–Cl_{br}–W′ and W–E–W′ (E = SPh or SePh) bond angles. Terminal chlorine atoms trans to bridging chlorine atoms have shorter W–Cl_t bond lengths, while those trans to the bridging chalcogens are longer.

Compounds **1**, **4**, and **5** contain tungsten–tungsten bond distances ranging from 2.69 to 2.79 Å. These distances are related to the major structural difference between the compounds, namely, different bridging ligands. Of the three compounds, $W_2Cl_6(dppm)_2$ (**5**)[5] with the relatively small bridging chlorine ligands possesses the shortest tungsten–tungsten bond length of 2.691 (1) Å. As one chlorine bridge is replaced by a bridging SePh group (**4**), where the atomic radius of selenium is greater than that for chlorine, the metal–metal bond becomes elongated to 2.708 (2) Å. This distance becomes even greater when both bridging chlorine atoms are replaced by SPh groups, as seen in compound **1** at 2.787 (1) Å. The more similar metal–metal bond distances for compounds **4** and **5** establish the smaller bridging ligand, chlorine, as the major influence on this distance. This is seen primarily by the small change in tungsten–tungsten bond length (0.017 Å) in going from **5** to **4** (one chlorine replaced) to the large difference (0.096 Å) is going from **5** to **1** (both chlorine bridges replaced).

Molybdenum Compounds. The structural features of $Mo_2(SPh)Cl_5(dppm)_2$ are very similar to those reported for $Mo_2Cl_6(dppm)_2$.[3b] The ORTEP diagram for **6** is shown in Figure 3. In both structures the angles around the two Mo centers are distorted from ideal octahedral geometry due to the presence of M–M bonding. For example the Mo–Cl_{br}–Mo angles for **6** and **7** are 70.79 (7) and 70.92 (5)°, respectively, Cl_{br}–Mo–S = 108.59 (3)° (**6**), Cl_{br}–Mo–Cl_{br} = 109.08 (5)° (**7**). The Mo–Mo distances of 2.788 (1) (**6**) and 2.789 (1) Å (**7**) are identical within experimental error. Replacement of one μ-Cl ligand with a μ-SPh group evidently has very little effect on the bonding properties of the Mo_2 unit. This is not surprising in view of the size similarity of sulfur and chlorine atoms.

Acknowledgment. We thank the National Science Foundation for support.

Registry No. **1**, 112533-49-0; **2**, 112548-88-6; **3**, 112533-50-3; **4**, 112548-90-0; **5**, 106297-42-1; **6**, 112533-52-5; **7**, 99808-51-2; $W_2Cl_4(dppm)_2$, 110796-27-5; $Mo_2Cl_4(dppm)_2$, 64508-35-6; PhSSPh, 882-33-7; PhSeSePh, 1666-13-3; CH_2Cl_2, 75-09-2; Cl_2, 7782-50-5.

Supplementary Material Available: For the crystal structures of $W_2(SPh)_2Cl_4(dppm)_2$, $W_2(SePh)Cl_5(dppm)_2$, and $Mo_2(SPh)Cl_5(dppm)_2$, full lists of bond distances, bond angles, and anisotropic displacement parameters (18 pages); lists of observed and calculated structure factors (72 pages). Ordering information is given on any current masthead page.

(12) Cotton, F. A.; Dunbar, K. D., manuscript in preparation.